Proceedings of 2012 IEEE
International Conference on Mechatronics and Automation
August 5 - 8, Chengdu, China

Unified Kinematics Modeling of Variable Topologies of a 3rT*PS* Metamorphic Parallel Mechanism

Hussam AlHussein and Dongming Gan[1]
Department of Mechanical Engineering
[1]*Khalifa University of Science, Technology & Research*
Abu Dhabi 127788, UAE
{100032394 & Dongming.gan}@kustar.ac.ae

Jorge Dias[1,3] and Lakmal Seneviratne[1,2]
[2]*King's College London, University of London*
[3]*University of Coimbra, Faculty of Science and Technology*
London WC2R2LS,UK
[3]Jorge.dias@kustar.ac.ae & [2] lakmal.seneviratne@kcl.ac.uk

***Abstract* - This paper investigates the mobility analysis and forward kinematics of 4 different configurations of 3(rt)PS parallel manipulators in which the moving platform and the base are two arbitrarily chosen platforms. After proposing mathematical model, multivariate polynomials describing the position and orientation of the moving platform are constructed in which the input data are the limb lengths, angels and design parameters. Based on the multivariate polynomials, a code was developed through Matlab Programming language utilizing the symbolic toolbox. It is shown that a maximum number of complete analytic solutions in complex and real domain for any input data is equal to 16. Numerical examples of forward displacement analysis of the 2 different configurations of the 3(rt)PS parallel mechanism are demonstrated to verify the analytic solutions. This special type of parallel mechanism paves the ground for the workspace, path planning and control of this special metamorphic mechanism.**

***Index Terms* - geometric constraint, reconfiguration, kinematics, parallel mechanisms**

I. INTRODUCTION

Parallel manipulators are relatively new field. The history goes back to Stewart Manipulator. In 1965 article [1], Stewart described his mechanism that has six degrees of freedom (DOF). In the recent years, parallel manipulators were investigated thoroughly due to their stiffness, load carrying capacity, good positioning accuracy and low inertia [2]. The analysis ranges from the forward and inverse kinematics to determining the singularities and actuator forces. Usually, a parallel manipulator of six DOF is not of high interest. Simpler mechanisms with lower and flexible degrees of freedom [3, 4] are increasingly becoming crucial for scientists and engineers.

The complexity of systems required the market to have metamorphic manipulator. Metamorphic parallel mechanisms (MPMs)[5] possess adaptability and flexibility to change the permanent mobility based on topological structure change. This change of the mobility by applying some geometrical constraints has plenty of advantages to the industry. It can serve some special workspace requirements and consequently, saves energy and money in the industry [5].

The metamorphic parallel mechanisms synthesized in this paper are based on a reconfigurable rT*PS* limb with two topology phases stemming from a reconfigurable Hooke (rT) joint [6]. Based on this rT joint, various metamorphic parallel mechanisms [5, 7] have been presented with a general construction method introduced using screw theory [7]. Using geometric constraints of the joints to change the constraint system of the mechanisms shows one way to obtain metamorphic mechanisms [8, 9] while the other way is to change the number of links by link coincidence and geometric constraint [10,11].

One of the configurations of the 3(rT)PS metamorphic parallel mechanism studied in this paper has similar topology with the 3RPS parallel mechanism. The 3RPS parallel manipulator is perhaps the most studied of defective parallel mechanisms [12]. The general 3RPS parallel mechanism was proposed by Hunt (1983) [13, 14, 15]. It has 3 degrees of freedom (DOF). The moving platform is connected to the fixed platform by means of three extendible limbs. The moving platform is connected to the limbs by three spherical joints while the lower body of the limb is connected by three revolute joints. The main difference between 3rT*PS* and 3R*PS* is that for the former one, the number of degrees of freedom can be modified to serve specific purposes.

In this paper, the focus is to analyse the 3(rT)*PS* parallel mechanism. This includes mobility analysis using screw theory for the different configurations. Since for each configuration can have different degrees of freedom, the workspace can be defined depending on the requirements of the operation. After that, the solution for both the forward and inverse displacement analysis are carried out for the general case of 3(rT)*PS* metamorphic manipulator by appealing to the sylvester's dialytic elimination method using Matlab-symbolic toolbox. It is shown that for all the different configurations we have same number of solution in the complex domain which equals to 16. Next, the numerical verification for the forward displacement analysis is computed for two configuration separately. Finally, figures of the real and positive solutions will be revealed as well.

In the following, the paper is arranged as: section 2 introduces the two phases of the rT*PS* limb with its geometric constraint analysis in screw theory; following this, mobility analysis of the 3rT*PS* metamorphic parallel mechanism is demonstrated section 3 and variable topologies are investigated in section 4; based on these, a unified kinematics

978-1-4673-1278-3/12/$31.00 ©2012 IEEE

modelling of the 3rT*PS* metamorphic parallel mechanism is proposed by covering all its topologies in section 5 with numerical examples illustrating the validity; conclusions are made in section 6.

II. TWO PHASES OF THE RECONFIGURABLE RTPS LIMB

The reconfigurable rT*PS* limb consists of a reconfigurable Hooke (rT) joint, a prismatic joint and a spherical joint. The reconfigurability of this limb stems from the configuration change of the rT joint which has two rotational degrees of freedom (DOFs) about two perpendicularly intersecting rotational axes (radial axis and bracket axis) as in Fig. 1. A grooved ring is used to house the radial axis and make it have the ability of altering its direction by rotating and fixing freely along the groove. This allows the radial rotation axis change with respect to the limb, resulting in two typical phases of the rT*PS* limb as in Fig. 1. While in Fig. 1(a), the radial axis is perpendicular to the limb (prismatic joint) which is denoted as $(rT)_1PS$, it is collinear with the limb (prismatic joint) passing through the spherical joint center in Fig. 1(b) and the limb phase is symbolized as $(rT)_2PS$.

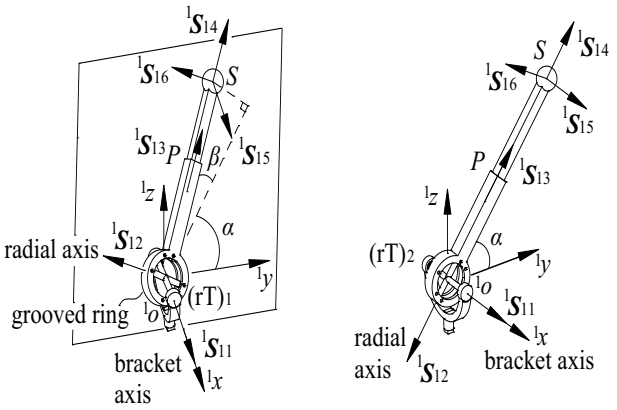

Figure 1 Two phases of the rT*PS* limb

Set a limb coordinate system ${}^1o{}^1x{}^1y{}^1z$ at the rT joint center with ${}^1x$ axis collinear with the bracket axis and ${}^1y$ axis perpendicular to the bracket surface as in Fig. 1(a), the twist system of the $(rT)_1PS$ limb is given as:

$$\left\{{}^1\boldsymbol{S}_1\right\}=\left\{\begin{array}{l}{}^1\boldsymbol{S}_{11}=[1\quad 0\quad 0\quad 0\quad 0\quad 0]\\ {}^1\boldsymbol{S}_{12}=[0\quad -s\alpha\quad c\alpha\quad 0\quad 0\quad 0]\\ {}^1\boldsymbol{S}_{13}=[0\quad 0\quad 0\quad -s\beta\quad c\beta c\alpha\quad c\beta s\alpha]\\ {}^1\boldsymbol{S}_{14}=[0\quad c\alpha\quad s\alpha\quad 0\quad ls\beta s\alpha\quad -ls\beta c\alpha]\\ {}^1\boldsymbol{S}_{15}=[1\quad 0\quad 0\quad 0\quad lc\beta s\alpha\quad -lc\beta c\alpha]\\ {}^1\boldsymbol{S}_{16}=[0\quad -s\alpha\quad c\alpha\quad lc\beta\quad ls\beta c\alpha\quad ls\beta s\alpha]\end{array}\right\}\qquad (1)$$

where, β is the angle between the limb (${}^1\boldsymbol{S}_{13}$) and its projection on plane ${}^1y{}^1o{}^1z$ passing through rT joint center and perpendicular to the bracket axis (${}^1x$), α is the angle between axis ${}^1y$ and the limb projection on plane ${}^1y{}^1o{}^1z$. l is the distance between the rT joint centre and the spherical joint centre. Labels cα and sα denote Cosine (α) and Sin (α) respectively. In the twist notation ${}^1\boldsymbol{S}_{ij}$, the first subscript i denotes the limb number, the second subscript j denotes the joint number within the limb and the leading superscript indicates the local frame.

The six screws in (1) form a six-system [15] and there is no reciprocal screw, showing that the $(rT)_1PS$ limb has six degrees of freedom (DOFs) and does not supply constraint to the platform connected to it.

For the $(rT)_2PS$ limb as in Fig. 1(b), radial axis of the rT joint is collinear with the prismatic joint passing through the spherical joint center. Thus, the spherical joint center A cannot move out of the plane ${}^1y{}^1o{}^1z$. Based on the coordinate system in Fig. 1(b)

It is clear that twists ${}^1\boldsymbol{S}_{12}$ and ${}^1\boldsymbol{S}_{14}$ are the same and the six twists form a five-system [15]. Thus, there is one reciprocal screw to (2) in the limb constraint system as

$$\left\{{}^1\boldsymbol{S}_1^r\right\}={}^1\boldsymbol{S}_1^r=\left[1\quad 0\quad 0\quad 0\quad ls\alpha\quad -lc\alpha\right]\qquad (2)$$

This gives a constraint force acting along a line passing through the spherical joint centre with a direction parallel to the bracket axis of the rT joint. Thus, the $(rT)_2PS$ limb has five DOFs, one less than the $(rT)_1PS$ phase.

III. THE 3RTPS MPM WITH PARALLEL CONSTRAINT SCREWS

A. Mobility analysis

From (2), It can be seen that $(rT)_2PS$ limb gives one constraint force to the platform with the direction parallel to its bracket axis. Thus, by arranging the direction of the bracket axis of the rT joint, the constraint to the platform can be represented. In this paper, the rT joints are connected to the base with parallel bracket axes, leading to parallel constraint forces expressed by screws on the platform as in Fig. 2.

Let points A_i and B_i denote the spherical joint center and the rT joint center in limb i (i=1,2,3) respectively. Locate a global coordinate system $oxyz$ at the center (B_1) of the rT joint in limb 1 with x axis collinear with the bracket axis and y axis perpendicular to the bracket plane. Let $\boldsymbol{a}_i$ and $\boldsymbol{b}_i$ denote the vectors of points A_i and B_i in the coordinate system $oxyz$, l_i be the distance between the spherical joint center A_i and the rT joint center B_i.

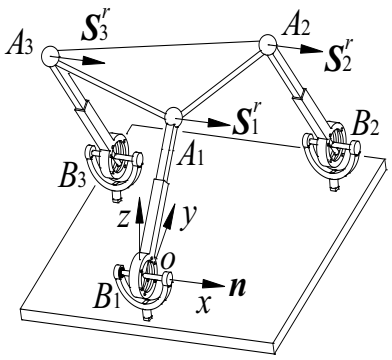

Figure 2 The 3(rT)$_2$PS with parallel constraint screws

The constraint system of the 3(rT)$_2$ *PS* parallel mechanism in Fig. 2 can be given as:

$$\{\boldsymbol{S}^r\} = \begin{Bmatrix} \boldsymbol{S}_1^r = [\boldsymbol{n} \quad \boldsymbol{a}_1 \times \boldsymbol{n}] \\ \boldsymbol{S}_2^r = [\boldsymbol{n} \quad \boldsymbol{a}_2 \times \boldsymbol{n}] \\ \boldsymbol{S}_3^r = [\boldsymbol{n} \quad \boldsymbol{a}_3 \times \boldsymbol{n}] \end{Bmatrix} = \begin{Bmatrix} [1 \;\; 0 \;\; 0 \;\; 0 \;\; l_1 s\alpha_1 \;\; -l_1 c\alpha_1], \\ [1 \;\; 0 \;\; 0 \;\; 0 \;\; b_{2z} + l_2 s\alpha_2 \;\; -b_{2y} - l_2 s\alpha_2] \\ [1 \;\; 0 \;\; 0 \;\; 0 \;\; b_{3z} + l_3 s\alpha_3 \;\; -b_{3y} - l_3 s\alpha_3] \end{Bmatrix} \quad (3)$$

where $\boldsymbol{n}$ = (1,0,0) is the direction of the bracket axes, $\boldsymbol{a}_i = \boldsymbol{b}_i + l_i(0, c\alpha_i, s\alpha_i) = (b_{ix}, b_{iy}, b_{iz}) + l_i(-s\beta_i, c\beta_i c\alpha_i, c\beta_i s\alpha_i)$, α_i is the angle between limb i and the line passing through rT joint center B_i with direction parallel to y axis, β_i is the angle between the limb and its projection on y-z plane passing through rT joint center and perpendicular to the bracket axis, here β_i =0 in the (rT)$_2$*PS* as in (3).

By taking reciprocal screws to (3), motion screws of the mechanism can be obtained as:

$$\{\boldsymbol{S}^r\} = \begin{Bmatrix} [1 \;\; 0 \;\; 0 \;\; 0 \;\; 0 \;\; 0] \\ [0 \;\; 0 \;\; 0 \;\; 0 \;\; 1 \;\; 0] \\ [0 \;\; 0 \;\; 0 \;\; 0 \;\; 0 \;\; 1] \end{Bmatrix} \quad (4)$$

which represent three DOFs with one rotation about x axis and two translations along y and z axes. Thus, the 3(rT)$_2$*PS* parallel mechanism with parallel constraint screws has mobility three with a rotation parallel to the screws and two translations perpendicular to the screws.

IV. Topology Reconfiguration

Altering the (rT)$_2$*PS* limbs in the 3(rT)$_2$*PS* parallel mechanism into the phase (rT)$_1$*PS* will result in various new mechanism topologies with increased mobility. After changing the phase of one limb, all the 3(rT)$_2$*PS* parallel mechanisms become the topology 2(rT)$_2$*PS*-1(rT)$_1$*PS* in Fig. 5(a) that has two parallel constraint screws following the first two in (4). One constraint less makes the 2(rT)$_2$*PS*-1(rT)$_1$*PS* one more DOF than the 3(rT)$_2$*PS*. Based on the constraint screw analysis, the 2(rT)$_2$*PS*-1(rT)$_1$*PS* parallel mechanism has four DOFs with two translations and two rotations (2R2T).

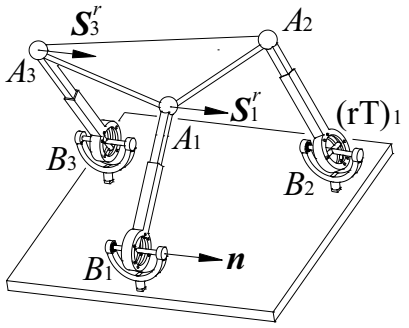

Figure 3 The 2(rT)PS-1(rT)1PS topology (4DOFs-2R2T)

When further changing one more limb phases, both the topologies in Fig.4(a) change to the same topology 1(rT)$_2$*PS*-2(rT)$_1$*PS* which has one constraint screw that limited the translation along $\boldsymbol{n}$. Thus, this mechanism has five DOFs with three rotations and two translations (3R2T).

When changing the third limb to phase (rT)$_1$*PS*, the mechanism becomes another topology 3(rT)$_1$*PS* as in Fig. 4(b) that does not have any constraint screw and has full mobility 6.

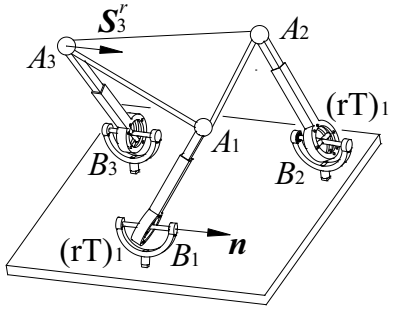

(a) 1(rT)$_2$*PS*-2(rT)$_1$*PS* (5DOFs-3R2T)

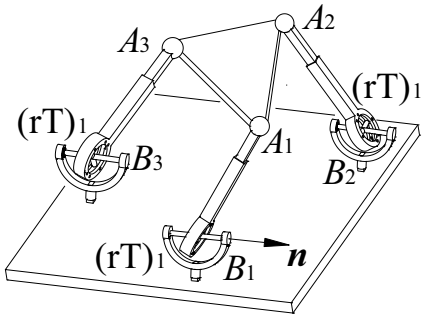

(b) 3(rT)$_1$*PS* (6DOFs)

Figure 4 Topologies 1(rT)$_2$*PS*-2(rT)$_1$*PS* and 3(rT)$_1$*PS*

V. KINEMATICS ANALYSIS

A. Inverse kinematics

The inverse displacement analysis of the 3rT*PS* metamorphic parallel mechanism is to obtain the actuation parameters (limb length l_i, radial-axis rotation angle β_i) based on the given platform position and orientation. Attach a local coordinate system *o*'*x*'*y*'*z*' at the line A1A2 of the platform with y' passing through A3 and perpendicular to **A1A2** as in Fig. 5.

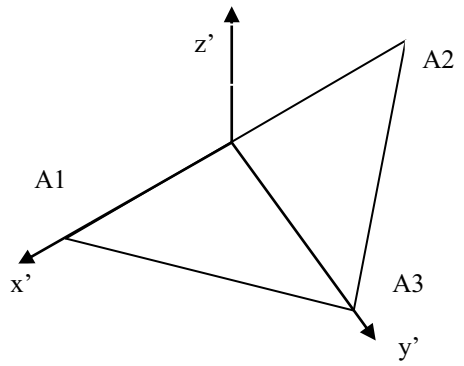

Figure 5 The platform coordinate system

When giving the platform position $\boldsymbol{p}$ (p_x, p_y, p_z) and orientation **R** described in the global coordinate system in Fig.5, the position of the spherical joint centers can be obtained as:

$$\begin{Bmatrix} \boldsymbol{a}_1 = \mathbf{p} + \boldsymbol{R}.(A1_{x'}, 0, 0) \\ \boldsymbol{a}_2 = \mathbf{p} + \boldsymbol{R}.(A2_{x'}, A2_{y'}, A2_{z'}) \\ \boldsymbol{a}_3 = \mathbf{p} + \boldsymbol{R}.(A3_{x'}, A3_{y'}, A3_{z'}) \end{Bmatrix} \tag{5}$$

where the spherical joint centers on the platform are randomly arranged on a triangular edges.

From (5), the inverse displacement analysis can be solved:

$$\begin{cases} l_1 = \sqrt{\boldsymbol{c}_1.\boldsymbol{c}_1}, \\ l_2 = \sqrt{\boldsymbol{c}_2.\boldsymbol{c}_2}, \\ l_3 = \sqrt{\boldsymbol{c}_3.\boldsymbol{c}_3}, \end{cases} \quad \begin{cases} \beta_i = \mathbf{sin}^{-1}(c_{iy}) & (\mathrm{rT})_1 PS \\ \beta_i = 0 & (\mathrm{rT})_2 PS \end{cases} \tag{6}$$

Where

$$\begin{cases} \boldsymbol{c}_1 = (\boldsymbol{a}_1 - \boldsymbol{b}_1) \\ \boldsymbol{c}_2 = (\boldsymbol{a}_2 - \boldsymbol{b}_2) \\ \boldsymbol{c}_3 = (\boldsymbol{a}_3 - \boldsymbol{b}_3) \end{cases}$$

c_{iy} is the element of vector $\boldsymbol{c}_i$ on the *y* axis, $\boldsymbol{a}_i$ is expressed in (5) and $\boldsymbol{b}_i$ is from (3).

B. Forward kinematics

On the contrary to the inverse displacement analysis, the forward one is to solve the platform position $\boldsymbol{p}$ (p_x, p_y, p_z) and orientation **R** when giving the corresponding actuation parameters (l_i, β_i) for each topology. Based on this and Fig.5, the geometric constraint of the platform triangle can be described as:

$$\begin{cases} d_{12}^2 = (\boldsymbol{a}_1 - \boldsymbol{a}_2)^2 \\ d_{13}^2 = (\boldsymbol{a}_1 - \boldsymbol{a}_3)^2 \\ d_{23}^2 = (\boldsymbol{a}_2 - \boldsymbol{a}_3)^2 \end{cases} \quad \begin{cases} \beta_i & (\mathrm{rT})_1 PS \\ \beta_i = 0 & (\mathrm{rT})_2 PS \end{cases} \tag{7}$$

Substituting each value of vector $\mathbf{a_i}$ belonging to the global coordinate into (5) and replacing

$\mathrm{Cos}(\alpha_i) = (1-t_i^2)/(1+t_i^2)$, $\sin(\alpha_i) = 2t_i/(1+t_i^2)$, there is

$$\begin{cases} f_1(1, t_1, t_1^2, t_2^2, t_1 t_2^2, t_1^2 t_2^2) = 0 \\ f_2(1, t_3, t_3^2, t_1^2, t_3 t_1^2, t_3^2 t_1^2) = 0 \\ f_3(1, t_2, t_2^2, t_3^2, t_2 t_3^2, t_2^2 t_3^2) = 0 \end{cases} \tag{8}$$

where $f_i(\bullet)$ is a linear function of the power product in the bracket with coefficients depending on known parameters only, t_i is $\mathrm{Tan}(\alpha_i/2)$.

By using Sylvester's dialytic elimination method [17] for the first two equations in (9), there is

$$f_4(1, t_3, t_2^2, t_3^2, t_2^2 t_3, t_3^3, t_2^4, t_3^4, t_2^2 t_3^2, t_2^2 t_3^3, t_2^4 t_3^1, t_2^2 t_3^4, t_2^4 t_3^2, t_2^4 t_3^3, t_2^4 t_3^4) = 0 \tag{9}$$

Where $f_4(\bullet)$ is a linear function of the power product in the bracket with coefficients depending on known parameters only.

Then, following the same method for (9) and the third equation in (8), a polynomial with only unknown t_3 can be obtained as:

$$\sum_{i=0}^{+16} h_i t_3^i = 0 \tag{10}$$

where the coefficient h_i are real constants depending on input data only.

This shows that an univariate equation in t_3 of degree 16 is obtained. Solving (10), sixteen solutions for t_3 can be obtained. Then, t_2 can be solved by substituting each solution of t_3 back to the third equation in (8) and selecting the roots satisfying (9). Following this, t_1 can be solved by substituting each pair of solutions of t_2 and t_3 into the first equation in (8) with proof of the second equation in (8). Based on this, sixteen pair of solutions of t_1, t_2, t_3 are obtained and the spherical joint center A_i can be calculated by substituting α_i=2ArcTan (t_i) into geometric constraint equation. Then, the platform position and orientation can be determined using the three spherical joint centers with Fig.5 as:

$$\begin{cases} \boldsymbol{z}' = (\boldsymbol{a}_2 - \boldsymbol{a}_1) \times (\boldsymbol{a}_3 - \boldsymbol{a}_1) / \| (\boldsymbol{a}_2 - \boldsymbol{a}_1) \times (\boldsymbol{a}_3 - \boldsymbol{a}_1) \| \\ \boldsymbol{x}' = (\boldsymbol{a}_1 - \boldsymbol{a}_2) / \| (\boldsymbol{a}_2 - \boldsymbol{a}_1) \| \\ \boldsymbol{y}' = (z' \times x') \\ \boldsymbol{R} = (x', y', z') \\ \boldsymbol{P} = \boldsymbol{a}_1 - d_{Ao} \boldsymbol{x}' \end{cases} \quad (11)$$

where d_{Ao}, is the distance between the local coordinate system of the moving platform to point A1.

VI. Numerical Examples of the Kinematics Analysis

From (10), the forward kinematics can be solved. As for each topology, there are sixteen, only the solutions for topology $3(rT)_2PS$ and $3(rT)_1PS$ are listed in Table 3 as an example. Real solutions of the chosen topologies are listed in table 3 with corresponding mechanism assemblies of the positive solutions are demonstrated in Fig. 6.

TABLE 1
Design Parameters

FIXED AND MOVING BASE	LOCATION
[U1 W1 Z1]	[0 0 0]
[U2 W2 Z2]	[1 3 0]
[U3 W2 Z3]	[-2 4 0]
L12	4.7176
L23	2.5461
L13	4.3944

TABLE 2
Input Parameters

Case	β_1	β_2	β_3	D1	D2	D3
1	0	0	0	10	13	12
2	10	7	5	10	13	12

TABLE 3
The Found Angles from the Forward Kinematics

	α_1	α_2	α_3
1	1.5595 -1.5595	1.4734 -1.4734	1.3976 -1.3976
2	1.0321 - 1.0321	1.2067 -1.2067	1.010394 -1.010394
3	1.5816	1.8696	1.37768
	-1.5816	-1.8696	-1.37768
4	1.273 -1.273	1.2383 -1.2383	0.991518 -0.991518
Case1 : $\beta_1 = \beta_2 = \beta_3 = 0$			
5	2.0686 -2.0686	1.9129 -1.9129	1.8853 -1.8853
6	1.0099 -1.0099	1.2144 -1.2144	1.09539 -1.09539
7	1.9338 -1.9338	2.2586 -2.2586	1.8516 -1.8516
8	1.4071 -1.4071	1.3271 -1.3271	0.997919 -0.997919
Case 2 : $\beta_1 \neq \beta_2 \neq \beta_3 \neq 0$			

In Fig. 6, the red triangles represent the base and the black lines represent the limbs, the platform coordinate system is shown with blue arrow in the ground plane direction.

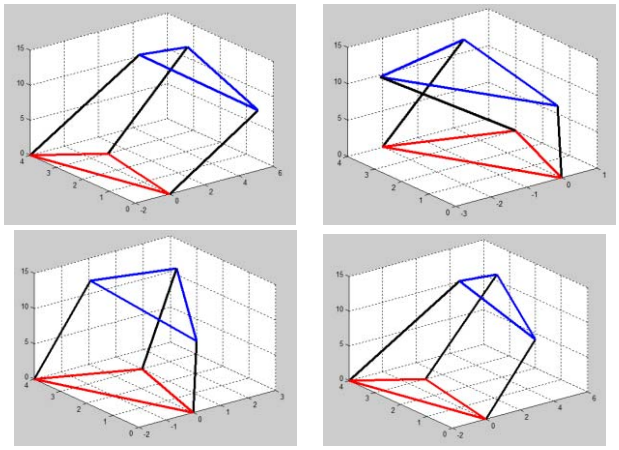

CASE 1 : $\beta_1 = \beta_2 = \beta_3 = 0$

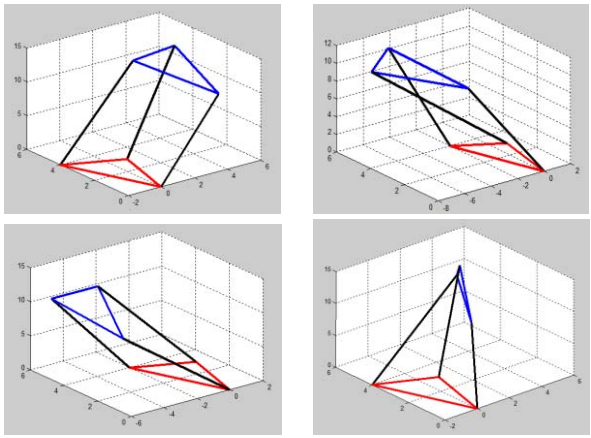

CASE2 : $\beta_1 \neq \beta_2 \neq \beta_3 \neq 0$

Figure 6 Configurations of the robot of two different cases

VII. CONCLUSION

This paper demonstrated the kinematics analysis of a new metamorphic mechanism consisting of four reconfigurable rTPS limbs. It was found that altering one of the three limb phases, the mechanism was changed to a new topology with mobility 4. Following this, by changing the limbs phases with different numbers and orders of the three limbs, the mechanism demonstrated various topologies with mobility change from 3 to 6. A unified kinematics solution was proposed by choosing a coordinate system on one of the rTPS joints and writing the constraint equations of the lengths of the moving platform. Although inverse kinematics was straight forward, however, forward kinematics involved complex procedure in the analytical solving with high-order polynomial equations. Unlike the mobility change, the number of solutions remains the same with the different configurations which equals to 16 in real and complex domain.

REFERENCES

[1] D. Stewart, "A Platform With Six Degrees of Freedom," *Journal of System Engineering and Control, Proc Inst. Mech*. Vol. 180, no.15 pp. 371–386, 1965

[2] J.P. Merlet, "*Parallel Robots*," 2nd Edition. Springer, 2008.

[3] L.W. Tsai, S.A. Joshi, Kinematic analysis of 3 DOF position mechanisms for use in hybrid kinematic machines, *ASME J. Mech. Des.*, 124(2) (2002) 245-253, 2002.

[4] Z. Huang, and Y.F. Fang, "Studying on the Kinematic Characteristics of 3-DOF in-Parallel Actuated Platform Mechanisms," Mech. Mach. Theory, **31**, pp. 1009–1018, 1996.

[5] D.M. Gan, J.S. Dai, and Q.Z. Liao, "Mobility analysis of two types of metamorphic parallel mechanisms,"*ASME Journal of Mechanisms and Robotics*, vol. 1, pp. 041007_1-9, 2009.

[6] D.M. Gan, J. S. Dai, Q.Z. Liao, "Constraint analysis on mobility change of a novel metamorphic parallel mechanism," *Mechanism and Machine Theory*, vol. 45 no. 12 , pp.1864-1876, 2009.

[7] D.M. Gan, and J.S. Dai, D.G. Caldwell, "Constraint-based limb synthesis and mobility-change aimed mechanism construction," *ASME J. Mech. Des.*,vol. 133, no. 5, pp. 051001_1-9, 2011.

[8] H.S. Yan and C.H., Kuo, "Topological representations and characteristics of variable kinematic joints," *ASME J. Mech. Des.*, vol. 128, no.2, pp. 384-391, 2006.

[9] K.T. Zhang, J.S. Dai, and Y.F. Fang, "Topology and constraint analysis of phase change in the metamorphic chain and its evolved mechanism," *ASME J. Mech. Des.*, vol. 132, no. 12, pp. 1-11, 2010.

[10] J.S. Dai, and J.J. Rees, "Mobility in metamorphic mechanisms of foldable/erectable kinds," *ASME J. Mech. Des.*, vol. 121, no. 3 pp. 375-382. 1999.

[11] J.S. Dai, and D. Wang, "Geometric analysis and synthesis of the metamorphic robotic hand," *ASME J. Mech. Des*., vol, 129 no. 11 pp 1191-1197. 2007.

[12] J. Gallardo, H. Orozco, and J.M. Rico, C.R. Aguilar and L. Perez "Acceleration Analysis of 3-RPS Parallel Manipulators by Means of Screw Theory, Parallel Manipulators," New Developments, Jee-Hwan Ryu (Ed.), ISBN:978-3-902613-20-2, InTech, Available from: http://www.intechopen.com/books/parallel_manipulators_new_developments, 2008.

[13] K.M. Lee, and D.K. Shah, "Kinematic analysis of a three-degree-of-freedom in-parallelactuated manipulator," *Proceedings IEEE International Conference on Robotics andAutomation,*vol. 1, pp. 345-350, 1987.

[14] C.H. Liu, and S. Cheng, "Direct singular positions of 3RPS parallel manipulators," *ASME Journal of Mechanical design* vol. 126, pp.1006-1016, 2004.

[15] K.T. Zhang, J.S. Dai, Y.F. Fang, Topology and constraint analysis of phase change in the metamorphic chain and its evolved mechanism, *ASME J. Mech. Des.*, vol. 132. no. 12. pp. 121001 pp. 1-11, 2010.

[16] M. Carricato, V. Parenti-Castelli, A family of 3-DOF translational parallel manipulators, *ASME J. Mech. Des*., vol. 125, no. 2, pp. 302–307. 2003

[17] Bottema, O., and Roth, B., Theoretical Kinematics, North-Holland, New York, 1979.